# Dalton Transactions

Accepted Manuscript

ROYAL SOCIETY OF CHEMISTRY

www.rsc.org/dalton

Journal Name RSCPublishing

ARTICLE

Cite this: DOI: 10.1039/x0xx00000x

Received 00th January 2012,
Accepted 00th January 2012

DOI: 10.1039/x0xx00000x

www.rsc.org/

# Nano-sized Mn oxide on halloysite or high surface area montmorillonite as an efficient catalyst for water oxidation with cerium(IV) ammonium nitrate: Supports from natural sources†

Mohammad Mahdi Najafpour[a,b*] and Emad Amini[a]

We used halloysite, a nano-sized natural mineral, and high surface area montmorillonite as supports for nano-sized Mn oxide to synthesize efficient water-oxidising catalysts. The composites were synthesized by an easy and simple procedure, and characterized by scanning electron microscopy, transmission electron microscopy, X-ray photoelectron spectroscopy, Fourier transform infrared spectroscopy, and X-ray diffraction spectrometry. Halloysite has low amounts of hydroxyl groups on its surface, thus it causes better dispersion of Mn oxides. The water-oxidising activities of these composites were also measured in the presence of cerium(IV) ammonium nitrate. Considering the low-cost, environmentally friendly precursors, simple synthesis and efficiency for water oxidation, the composites are promising catalysts in artificial photosynthetic systems.

## Introduction

Electrochemical or photoelectrochemical water splitting to high scale $H_2$ production is a promising route for the conversion of sustainable, but intermittent energies.[1] Efficient light harvesting compounds, charge separation and catalysts are necessary in this procedure.[1] Among different reactions, water oxidation is a bottleneck for water splitting into $H_2$ and $O_2$ and thus, the finding of an efficient, cheap and environmentally friendly water-oxidising compound is highly desirable for artificial photosynthetic systems.[1] Among different compounds,[2] Mn complexes[3] are very interesting because they are not only cheap and environmentally friendly, but also Nature[4] uses a Mn oxido cluster for water oxidation. However, a few manganese complexes have been reported as true catalyst for water oxidation.[5] Many Mn complexes are decomposed, or are not true catalysts for water oxidation in the presence of oxidants.[6] Mn oxides are true catalysts in some water-oxidation reactions by Mn-based catalysts.[6]

In 1968, Glikman and Shcheglova reported water-oxidising activirty of Mn oxides in the presence of cerium(IV) ammonium nitrate (Ce(IV)) as an oxidant.[7] In the next step, Morita in 1977 showed electrochemical water oxidation by the compounds.[8] Then, Shilov extended the water-oxidising activity of Mn oxides in different conditions.[9] Harriman's group in 1988 indicated that cobalt, iridium, manganese(III) and ruthenium oxides are efficient catalysts for water oxidation in the presence of Ce(IV) or $Ru(bpy)_3^{3+}$ as chemical oxidant.[10] The group also reported calcination temperature and different supports as important factors in water oxidation.[10] After these studies, different Mn oxides were introduced as efficient catalysts toward water oxidation.[11]

Gold particles on Mn oxides improve their activity towards water oxidation.[12] Nanostructured Mn oxide clusters supported on mesoporous silica in the presence of $Ru(bpy)_3^{3+}$ was reported by Jiao and Frei.[13] Jiao and Frei also suggested that the support stabilised the catalyst and facilitated proton transfer.

In 2013, Dismukes' group prepared very pure β-$MnO_2$, R-$MnO_2$, α-$MnO_2$, δ-$MnO_2$, λ-$MnO_2$, $LiMn_2O_4$, $Mn_2O_3$, and $Mn_3O_4$. They reported that the $Mn_2O_3$ and $Mn_3O_4$ are among the most active Mn oxides for water oxidation.[14] Recently, Najafpour's group showed that different Mn oxide phases in the presence of Ce(IV) or in electrochemical water oxidation convert to a layered Mn oxide after a few hours.[15] Such nanolayered Mn oxides have no long-range order and could be considered as disordered Mn oxides. Self-healing for Mn oxides were also reported.[16] In the self-healing reaction, decomposition products from Mn oxide in the water-oxidation reaction can react or combine to remake Mn oxide and is very important in stability of Mn oxides.[16] Mn oxide/carbon nanotubes (CNT), graphene (G), graphene oxide (GO), $C_{60}$ and nanodiamond were shown as promising composites for water oxidation.[17]

Nakmura's group reported that the treatment by amines stabilizes Mn(III) ions on the surface of Mn oxides and increases the water-oxidising activity of the Mn oxides efficiently.[18,19]

As discussed by Nocera, the population of electrons in antibonding orbitals of metal oxide, $e_g^*$ and $t_{2g}^*$, decreases the M−O bond order and lead to decomposition. Thus, decomposition even under acidic conditions for early first-row transition metal oxides, such as $MnO_x$, is lower than the late first-row metal oxides.[20] The Nocera group also reported that the Mn oxide is stable under the water oxidation conditions up to 4 M HCl due to self-healing..[20]

The promising water oxidation and oxygen reduction catalysed by α, β, δ-$MnO_2$ or amorphous Mn oxide were investigated systematically in alkaline media by Suib's group.[21]

New applications of natural minerals are interesting and promising area of science. Here, we considered halloysite as a support for Mn oxide. Halloysite has a nanostructure with a tubular shape that facilitates its use as a support for various catalysts. The nanotubes have typical dimensions of, 10-50 nm in outer diameter, 5-20 nm in inner diameter with 2-40 mm in length. Halloysite can be recovered from various deposits from China, New Zealand, America, Brazil, and France.[22] Its applications contain remediation of environmental contaminants, the delivery of drugs and various macro molecules, storage of molecular hydrogen and for catalytic conversion and processing of hydrocarbons, the fabrication of high quality ceramic white-ware, nano-templates, and support for different catalysts.[22]

Herein, we consider Mn oxide on halloysite and high surface area montmorillonite as water-oxidising catalysts.

## Experimental

### Material and methods

Halloysite (64 $m^2/g$) and high surface (250 $m^2/g$) montmorillonite were purchased from Sigma-Aldrich. All reagents and solvents were purchased from commercial sources and were used without further purification. SEM was carried out with LEO 1430VP device. The X-ray powder patterns were recorded with a Bruker D8 ADVANCE diffractometer ($CuK_\alpha$ radiation). Mn atomic absorption spectroscopy (AAS) was performed on an Atomic Absorption Spectrometer Varian Spectr AA 110. Prior to the analysis, the composites were added to of concentrated nitric acid (1 mL) and $H_2O_2$ (0.2 mL, 30%) , then left at room temperature for at least 1 h to ensure that the oxides were completely dissolved. The solutions were then diluted to 25.0 mL and analysed by AAS.

### Synthesis

A simple procedure was used to synthesize the composites:

A solution of $KMnO_4$ (200 mg in 60 mL water) was added to 2.0 g high surface area montmorillonite or halloysite. The mixture was placed under hydrothermal condition at 120 °C for 12 h. The solid was centrifuged, and washed with water to remove $KMnO_4$. Then, the brown solid was dried at 60 °C in air. The solid was calcined at at the appropriate temperature for some experiments.

### Water oxidation

Oxygen evolution from aqueous solutions in the presence of Ce(IV) was investigated using an HQ40d portable dissolved oxygen-meter connected to an oxygen monitor with digital readout. The reactor was maintained at 25.0 ºC in a water bath. In a typical run, the instrument readout was calibrated against air-saturated distilled water stirred continuously with a magnetic stirrer in the air-tight reactor. After ensuring a constant baseline reading, water in the reactor was replaced with Ce(IV) solution. Without the catalyst, Ce(IV) was stable and oxygen evolution was not observed. After deaeration of the Ce(IV) solution with argon or nitrogen, Mn oxides as powder were added, and oxygen evolution was recorded with the oxygen meter under stirring (Scheme 1). The formation of oxygen was followed and the oxygen formation rates per Mn site were obtained from linear fits of the data by the initial rate. Water oxidation was performed by a set up shown in Scheme S1 (ESI†).

## Results and discussion

Nano-sized Mn oxide on halloysite or high surface area montmorillonite was synthesized by a simple method using low-cost and environmentally friendly method. The composites were synthesized by the reaction of $MnO_4^-$ ions and halloysite or montmorillonite. The details of the reaction are not known, however, we propose that the decomposition of $MnO_4^-$ occurs on the surface of halloysite or montmorillonite under hydrothermal conditions:

$4MnO_4^- + 4H^+ \rightarrow 4MnO_2 + 3O_2 + 2H_2O$

It is possible that AlOH or SiOH on the surface of the supports induces the decomposition of the $MnO_4^-$ ion and nano-sized $MnO_2$ precipitates slowly on the surface of the supports. These supports are stable under the synthetic conditions and in contrast to nano carbon structures, do not serve as sacrificial reductants in the conversion of $MnO_4^-$ to Mn oxide.

In the FTIR spectra, a broad band at ~ 3200 - 3500 $cm^{-1}$ is observed that is related to antisymmetric and symmetric O-H stretchings. H-O-H bending from water can be observed at ~ 1630 $cm^{-1}$ (Fig. S1-S6, ESI†).[23] However, the peaks related to $MnO_6$ cores were not observed because of low amounts of Mn oxide in the composites. The 1040-1100 $cm^{-1}$ peaks are related to the stretching mode of Si-O, and the band at 1030 $cm^{-1}$ was caused by the stretching vibration of Si-O-Si. The bands at 520-540 $cm^{-1}$ was assigned to the vibration of Al-O-Si.[23a]

As previously reported, XRD is used to both characterize halloysite and determine dehydrated or hydrated forms of the composites. The hydrated halloysite exhibits a 10 Å spacing of the layers and the space for the dehydrated (meta-halloysite) is 7 Å.[23] In other words, regarding hydration, there are two forms for halloysite: The hydrated form is $Al_2Si_2O_5(OH)_4.2H_2O$ (10 Å) with and the dehydrated form is $Al_2Si_2O_5(OH)_4$ (7 Å).[23] The interlayer water in the hydrated form is held weakly.[23] Thus, 10 Å halloysite is usually found in humid regions, but in dry climates, 7 Å halloysite is formed.[23] According to XRD, the peak at 12° (2θ) is related to a (001) basal spacing of 7 Å (Fig. 1).[23] A peak at 8.8° (2θ) shows the 10 Å form, which is indicative of hydrated halloysite. As shown in Fig. 1, at 100 ºC more crystalinity is observed than for the original halloysite.[23] However, as the temperature is increased, the structure of halloysite disintegrates due to the slow disappearance of the lattice water. Details for XRD patterns for halloysite and montmorillonite are reported in ESI (Fig. S7-S13, ESI†). The Mn oxides are amorphous in these conditions, and no pattern related to Mn oxide is observed.

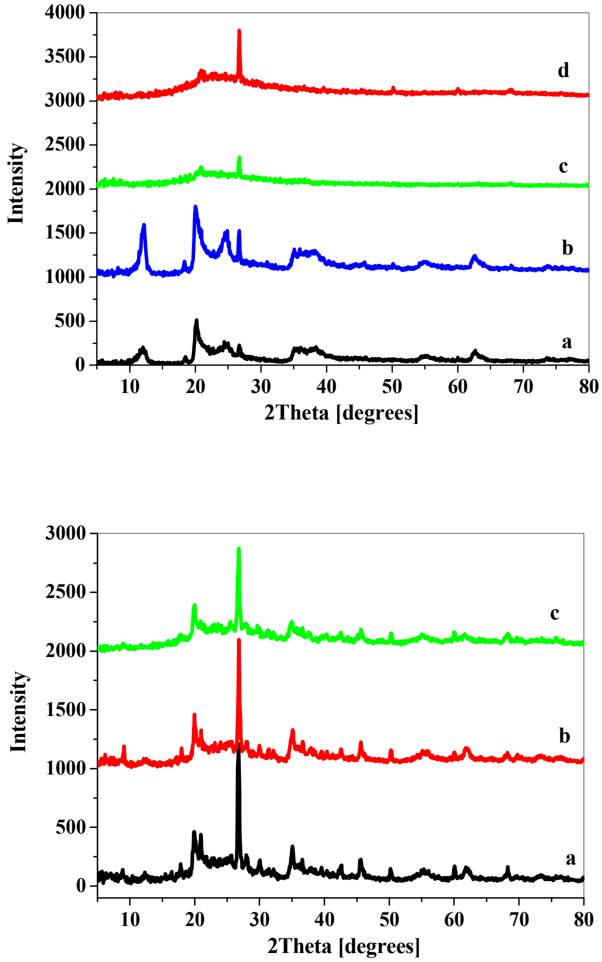

Fig. 1 Top: XRD patterns of nano-sized Mn oxide on halloysite. Halloysite (a), nano-sized Mn oxide on halloysite calcined at 100 (b), 400 (c) and 500 ºC (d). Below: XRD patterns of montmorillonite (a), and nano-sized Mn oxide on montmorillonite calcined at 100 (b) and 500 ºC (c).

Although amounts of Mn oxides on the surface of halloysite were low, Mn oxide on the surface of halloysite could be also considered by X-ray photoelectron spectroscopy (XPS). The Mn $2p_{3/2}$ (640) and $2p_{1/2}$ (649) binding energy of the coating was consistent with that of Mn(III) (Fig. 2).[23b]

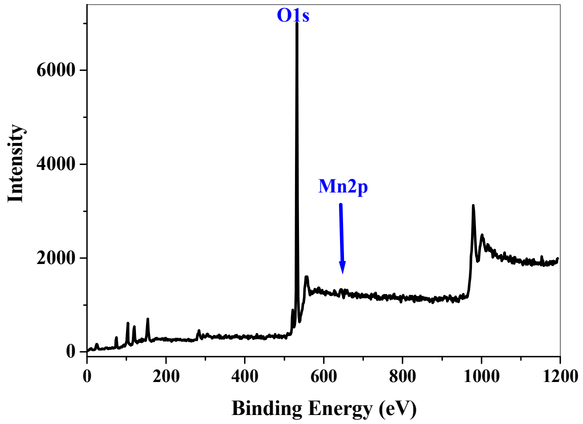

a

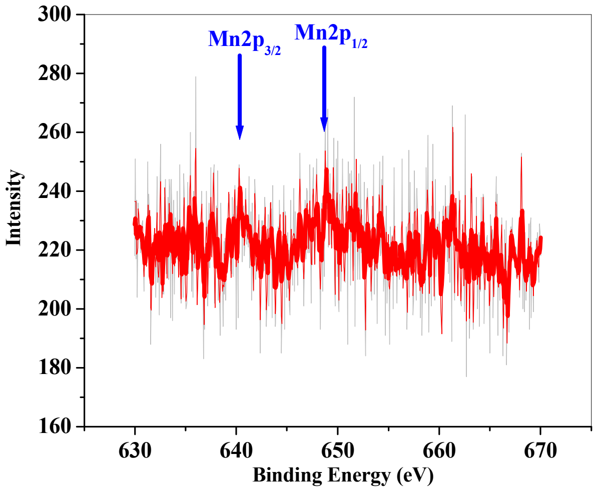

b

Fig. 2 XPS for nano-sized Mn oxide on halloysite (a,b). The related peaks for Mn are shown by blue arrows (b).

To characterize the morphology of the prepared oxides, they were studied by scanning electron microscopy (SEM).

SEM images are shown in Fig. 3a,b (also see Fig. S14-S17, ESI†). These images from halloysite show nanotube with dimension of 30-100 nm × 30-70 nm × 300-500 nm. In SEM images for montmorillonite or Mn oxide on montmorillonite, sheets are observed (Fig. 3c,d). TEM images (Fig. 3e-h) show nano-sized Mn oxides on the surface of supports. Although, as shown in images, amount of Mn oxides on the surface of halloysite is lower than amount of Mn oxide on the surface of montmorillonite. This result consists with the results of AAS, which indicates amount of Mn oxides per gram of support is ~ 5 times more for montmorillonite.

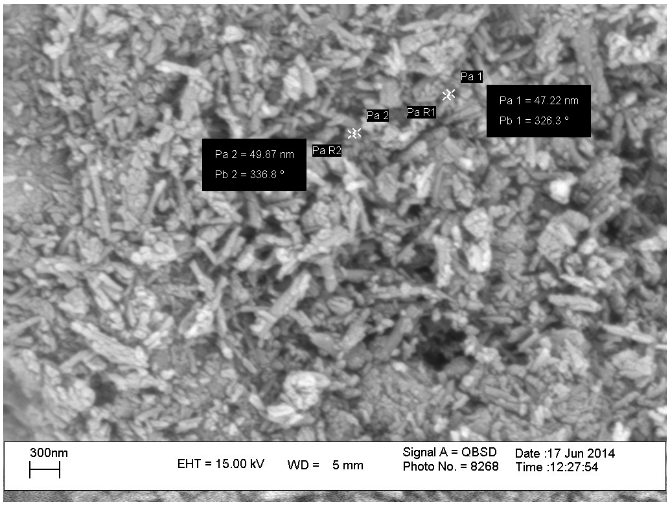

a

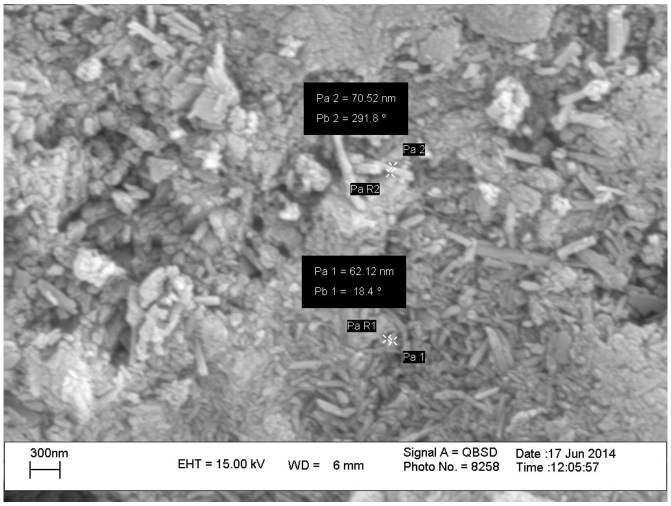
Pa 2 = 70.52 nm
Pb 2 = 291.8 °
Pa 2
Pa R2
Pa 1 = 62.12 nm
Pb 1 = 18.4 °
Pa R1
Pa 1
300nm
EHT = 15.00 kV
WD = 6 mm
Signal A = QBSD
Photo No. = 8258
Date :17 Jun 2014
Time :12:05:57

b

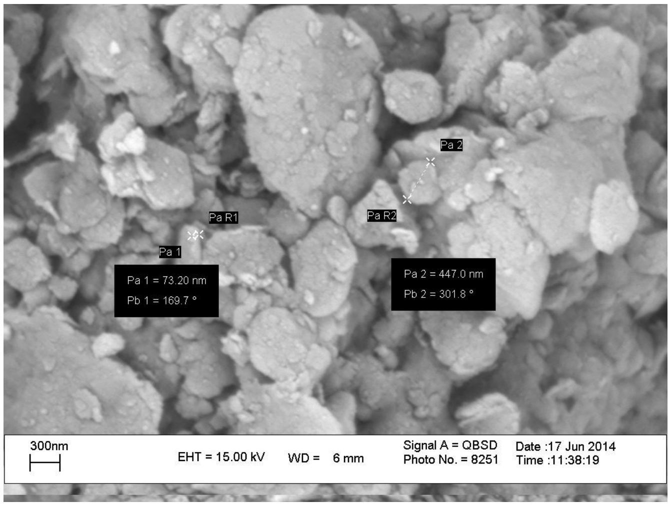
Pa 2
Pa R1
Pa R2
Pa 1
Pa 1 = 73.20 nm
Pb 1 = 169.7 °
Pa 2 = 447.0 nm
Pb 2 = 301.8 °
300nm
EHT = 15.00 kV
WD = 6 mm
Signal A = QBSD
Photo No. = 8251
Date :17 Jun 2014
Time :11:38:19

c

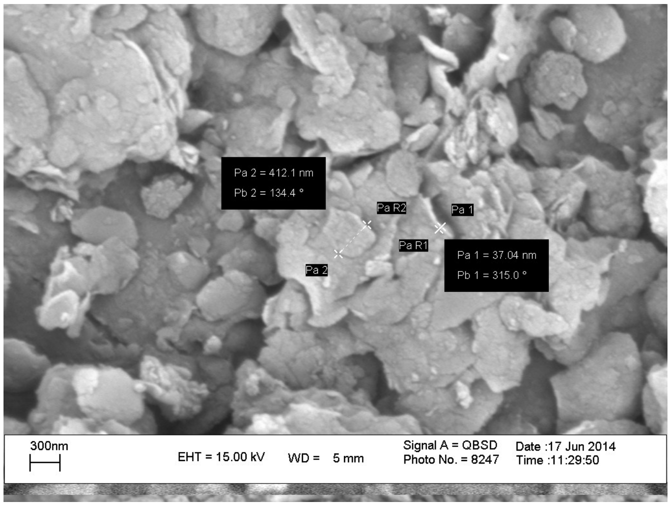
Pa 2 = 412.1 nm
Pb 2 = 134.4 °
Pa R2
Pa 1
Pa R1
Pa 2
Pa 1 = 37.04 nm
Pb 1 = 315.0 °
300nm
EHT = 15.00 kV
WD = 5 mm
Signal A = QBSD
Photo No. = 8247
Date :17 Jun 2014
Time :11:29:50

d

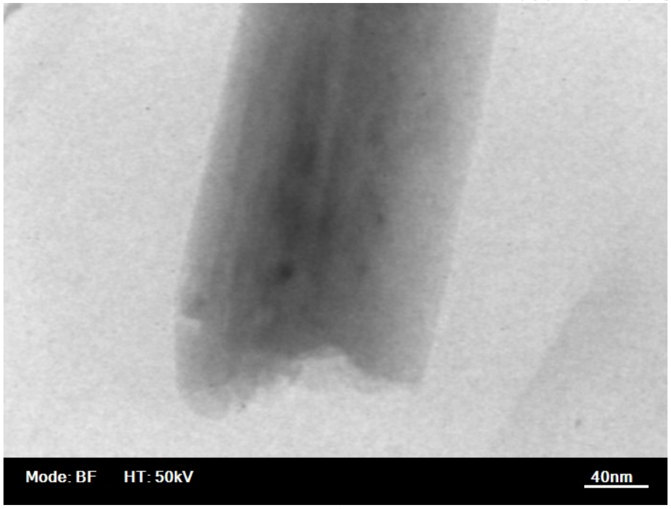
Mode: BF
HT: 50kV
40nm

e


Mode: BF
HT: 50kV
20nm

f

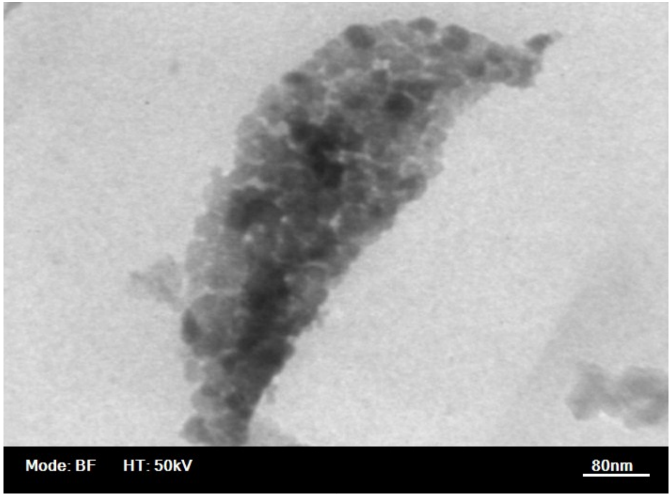
Mode: BF
HT: 50kV
80nm

g

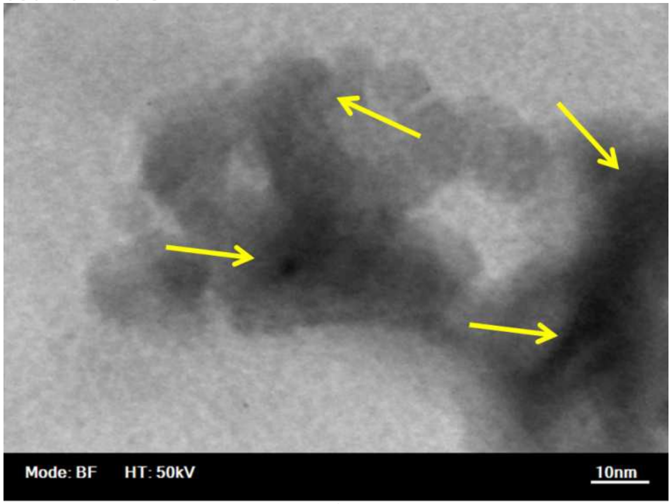

h

Fig. 3 SEM images of halloysite (a), nano-sized Mn oxide on halloysite (b), montmorillonite (c) and nano-sized Mn oxide on montmorillonite (d). TEM images from nano-sized Mn oxide on halloysite (e,f) or montmorillonite (g,h).

In the next step, we studied the water-oxidation activity of these composites in the presence of Ce(IV). The first, the effect of calcination temperature on water-oxidising activity was considered (Fig. 4a). The calcination temperature has an important effect on the water-oxidation catalysis of the Mn oxide on halloysite and in the range of 200-400 °C, the composites convert to an efficient water-oxidising catalyst. However, at high calcined temperatures, water-oxidising activity decreases. Similar effects have been observed for other Mn oxides. With the montmorillonite, the calcination temperature has little effect on the water-oxidation catalysis of the Mn oxides within the range 200-400 °C.

The turnover frequencies (TOFs) for different amounts of both catalysts are very similar. It means that the rate of oxygen evolution increases linearly with the amounts of catalyst (Fig. 4b).

In the next step, we studied the effect of concentration of Ce(IV) on the water-oxidation reaction. The reactions were done with different concentrations of Ce(IV) keeping all other factors constant as shown in Fig. 4c. The effects of Ce(IV) concentration is complicated due to both water oxidation and catalyst decomposition at high Ce(IV) levels. For nano-sized Mn oxide on halloysite, different water-oxidising activities are not observed with different concentrations of Ce(IV). However, with 0.55 M Ce(IV) greater water water-oxidising activity is observed. On montmorillonite, the concentration of Ce(IV) has little effect on the rate of catalytic water oxidation by nano-sized Mn oxides.

In the water-oxidation condition without montmorillonite or halloysite no oxygen evolution was observed (Fig. S20, ESI†).

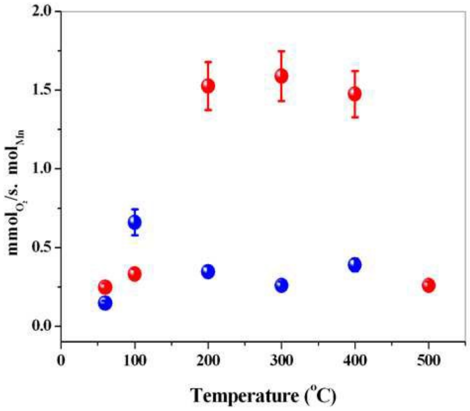

a

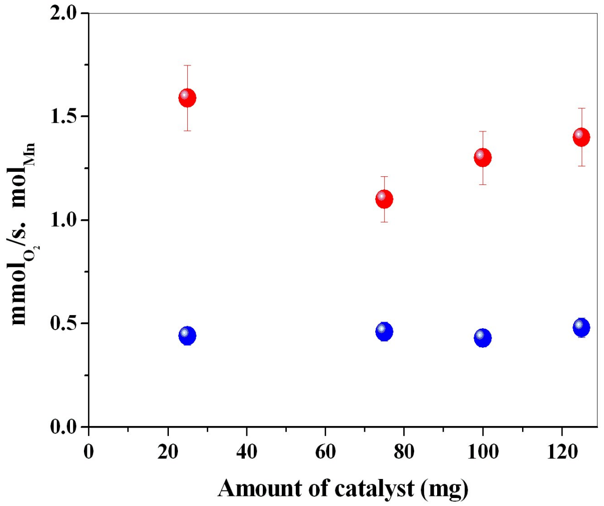

b

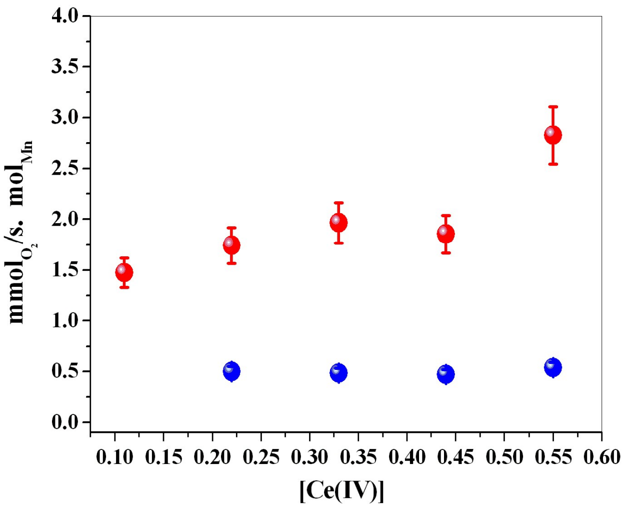

c

Fig. 4 Oxygen evolution of an aqueous solution of Ce(IV) (40 mL, 0.11 M) at 25.0 °C in the presence of nano-sized Mn oxide on halloysite (red) or high surface area montmorillonite (blue) (a). Oxygen evolution of an aqueous solution of Ce(IV) (40 mL, 0.11) at 25.0 °C in the presence of different amounts of nano-sized Mn oxide on halloysite (red) or high surface area montmorillonite (blue) calcined at 400 and 100 °C, respectively (b). Oxygen evolution of an aqueous solution of Ce(IV) with different concentrations of Ce(IV) at 25.0 °C in the presence of nano-sized Mn oxide on halloysite (red) or high surface area montmorillonite (blue) calcined at 400 and 100 °C, respectively (b).

Comparing with other Mn oxides (Table 1), nano-sized Mn oxide on halloysite is amongst the most efficient catalysts toward water oxidation in the presence of chemical oxidant with TOF ~ 1.5-2.8. The nano-sized Mn oxide on high surface area montmorillonite is also a good catalyst for water oxidation (TOF ~ 0.5). Under the conditions used for water oxidation the Mn oxides supported on halloysite or high surface are montmorillonite are more stable than on carbon nanotube supports. In other words, although nano carbons can improve electron transfer, they are less stable than nano-$SiO_2/Al_2O_3$ structures. On the other hand, halloysite and montmorillonite, in contrast to many nano carbons, are low-cost and non-toxic.

Table 1 The rate of water oxidation by the various Mn based catalysts for water oxidation in the presence of non-oxygen transfer oxidant chemical oxidants.

Compared with other silicates such as kaolinite and montmorillonites, halloysite has a low density of surface hydroxyl groups. Such low densities of hydroxyl groups on the surface causes better dispersion of Mn oxides than other silicate.[22] AAS and TEM images show that the amount of Mn oxides on the surface of montmorillonite and halloysite are ~ 1% and 0.2 %, respectively. Thus, Mn oxide on the surface of montmorillonite is~ 5 times more than Mn oxides on the surface of halloysite. Such low amounts of Mn oxide on the surface of halloysite cause smaller/thinner Mn oxides, which are more efficient in water oxidation. On the other hand, this higher loading effect may be due to the clay mineral being acid activated to increase the surface is allowing larger $MnO_x$ crystals to form on the macro-/meso-porous surface. The large crystals, no-longer being nano-sized will be less active as catalysts, possibly explaining the lower activity of the montmorillonite supported catalyst. To find long-term stability of catalysts, we analyzed amounts of Mn in a solution of Ce(IV) (0.11 M) after different times (Fig. 5). As shown in Fig. 5, high decomposition of Mn oxide supported on montmorillonite occurs in this condition but lower decomposition of Mn oxide supported on halloysite was observed in this condition.

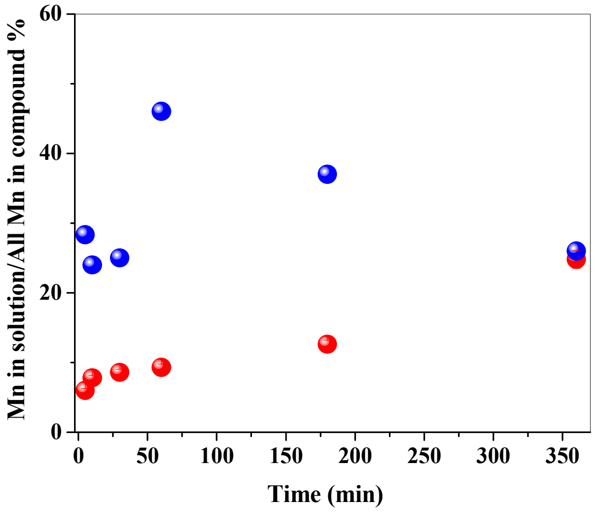

Fig. 5 Amounts of Mn in solution to all Mn in Mn oxides supported montmorillonite (blue) and halloysite (red) in the presence of Ce(IV) (0.11 M) after different times.

In water splitting systems, largescale deployment issue is very important and even cobalt with its high importance for battery components is now believed as a critical material in according to its significant supply risks for largescale deployment.[46,47] Thus, efficient, environmentally friendly, low-cost and available Mn-based catalysts such as Mn oxides and supports such as $SiO_2$ are promising in artificial photosynthesis. On the other hand, morphologies and structures of supports are also important to improve catalytic activity of catalyst. Such catalysts can be used in the presence of chemical oxidant, photochemical and electrochemical conditions.

## Conclusions

We synthesized nano-sized Mn oxide on halloysite or high surface area montmorillonite by a simple method. Nano-sized Mn oxide on halloysite is an efficient catalyst toward water oxidation (TOF ~ 1.5-2.8), and nano-sized Mn oxide on high surface area montmorillonite is reasonable catalyst for this catalytic reaction (TOF ~ 0.5). We also studied the effect of amount of catalysts, concentration of Ce(IV) and calcination temperatures on water-oxidation reaction of these catalysts. The effect of amount of catalysts and the concentrations of Ce(IV) on water-oxidising activities of these catalysts were small. However, calcination temperature was an important factor for the efficiency of the catalysed process with $MnO_x$ on halloysite. In contrast to nano carbon structures, both halloysite and high surface area montmorillonite as supports are stable under the water-oxidising condition. Halloysite has been used as a support for a variety of catalysts for different reactions,[22,45] we suggest that the mineral is also a promising support for other oxidation catalysts due to its stability, low cost and its being environmentally. Halloysite has a low density of surface hydroxyl groups, thus giving better dispersion of Mn oxides than other silicates. The results show that supports have important effect to improve water-oxidizing activity of Mn oxide toward water oxidation. A challenge in future is synthesis of stable Mn oxide on such supports.

## Acknowledgements

The authors are grateful to the Institute for Advanced Studies in Basic Sciences and the National Elite Foundation for financial support.

## Notes and references

[a]*Department of Chemistry, Institute for Advanced Studies in Basic Sciences (IASBS), Zanjan, 45137-66731, Iran*
[b]*Center of Climate Change and Global Warming, Institute for Advanced Studies in Basic Sciences (IASBS), Zanjan, 45137-66731, Iran*
**Corresponding author; Phone: (+98) 24 3315 3201; E-mail: mmnajafpour@iasbs.ac.ir*

† Electronic Supplementary Information (ESI) available: [details of any supplementary information available should be included here]. See DOI: 10.1039/c000000x/

1 H. B. Gray, *Nat. Chem.*, 2009, **1**, 7; M. Armand , J. M. Tarascon , *Nature*, 2008, **451**, 652; A. Paracchino, V. Laporte, K. Sivula, M. Grätzel and E. Thimsen, *Nat. Mater.*, 2011, **10**, 456; H. Thomas, Y. Bozec, K. Elkalay and H. J. W. De Baar, *Science*, 2004, **304**, 1005; V. R. Stamenkovic, B. Fowler, B. S. Mun, G. Wang, P. N. Ross, C. A. Lucas and N. M. Markovic, *Science*, 2007, **315**, 493; F. E. Osterloh, *Chem. Soc. Rev.*, 2013, **42**, 2294.

2 A. Singh, L. Spiccia, *Coord. Chem. Rev.*, 2013, **257**, 2607; X. Liu and F. Wang, *Coord. Chem. Rev.*, **256**, 1115.

3 M. M. Najafpour and S. I. Allakhverdiev, *Int. J. Hydrogen Energy*, 2012, **37**, 8753; W. Ruttinger and G. C. Dismukes, *Chem. Rev.*, 1997, **97**, 1; M. Yagi and M. Kaneko, *Chem. Rev.*, 2001, **101**, 21; H. J. M. Hou, *J. Integr. Plant. Biol.*, 2010, **52**, 704; H. J. M. Hou, *Materials*, 2011, **4**, 1693; K. Beckmann, H. Uchtenhagen, G. Berggren, M. F. Anderlund, A. Thapper, J. Messinger, S. Styring and P. Kurz, *Energy Environ. Sci.*, 2008, **1**, 668; M. Hirahara, A. Shoji and M. Yagi, *Eur. J. Inorg. Chem.*, 2014, **4**, 595.

4 V. K. Yachandra, V. J. DeRose, M. J. Latimer, I. Mukerji, K. Sauer and M. P. Klein, *Science*, 1993, **260** 675; J. E. Penner-Hahn, Structural characterization of the Mn site in the photosynthetic oxygen-evolving complex, in: H. A. O. Hill, P. J. Sadler, A. J. Thomson (Eds.), Metal Sites in Proteins and Models: Redox Centres, vol. 90, Springer, Berlin /Heidelberg, Germany, 1998, pp. 1-36; H. Dau, L. Iuzzolino and J. Dittmer, *Biochim. Biophys. Acta*, 2001, **1503**, 24; K. Sauer, J. Yano and V. K. Yachandra, *Coord. Chem. Rev*., 2008, **252**, 318; A. Zouni, H. T. Witt, J. Kern, P. Fromme, N. Krauss, W. Saenger and P. Orth, *Nature*, 2001, **409**, 739; N. Kamiya and J.-R. Shen, *Proc. Natl. Acad. Sci. USA.*, 2003, **100**, 98; K. N. Ferreira, T. M. Iverson, K. Maghlaoui, J. Barber and S. Iwata, *Science*, 2004, **303**, 1831; B. Loll, J. Kern, W. Saenger, A. Zouni and J. Biesiadka, *Nature*, 2005, **438**, 1040; J. Yano, J. Kern, K. Sauer, M. J. Latimer, Y. Pushkar, J. Biesiadka, B. Loll, W. Saenger, J. Messinger and A. Zouni, *Science*, 2006, **314**, 821; J. W. Murray, K. Maghlaoui, J. Kargul, N. Ishida, T.-L. Lai, A. W. Rutherford, M. Sugiura, A. Boussac and J. Barber, *Energy Environ. Sci*., 2008, **1**, 161; K. Kawakami, Y. Umena, N. Kamiya and J. R. Shen, *Proc. Natl. Acad. Sci. USA.*, 2009, **106**, 8567; A. Guskov, J. Kern, A. Gabdulkhakov, M. Broser, A. Zouni and W. Saenger, *Nat. Struct. Mol. Biol.*, 2009, **16**, 334; M. Broser, C. Glöckner, A. Gabdulkhakov, A. Guskov, J. Buchta, J. Kern, F. Müh, H. Dau, W. Saenger and A. Zouni, *J. Biol. Chem*., 2011, **286**, 15964; S. I. Allakhverdiev, *Photosynth. Res*., 2008, **98**, 1; S. I. Allakhverdiev, *J. Photochem. Photobiol. B*, 2011, **104**, 1; E. M. Sproviero, J. A. Gascón, J. P. McEvoy, G. W. Brudvig and V. S. Batista, *J. Am. Chem. Soc*., 2008, **130**, 3428; M. M. Najafpour, *Plant Biosyst*., 2006, **140**, 163; M. M. Najafpour, *Origins Life Evol. Biosphere*, 2009, **39**, 151; G. Renger, *Biochim. Biophys. Acta*, 2001, **1503**, 210; M. M. Najafpour, M. Abasi and S. I. Allakhverdiev, *NanoPhotoBioSciences*, 2013, **1**, 79. Y. Umena, K. Kawakami, J. R. Shen and N. Kamiya, *Nature*, 2011, **473**, 55. Y. Umena, N. Kamiya and J. R. Shen, *J. Photochem. Photobiol. B*, 2011, **104**, 9; M. Wiechen, M. M. Najafpour, S. I. Allakhverdiev and L. Spiccia, *Energy Environ. Sci*., 2014, **7**, 2203.

5 E. A. Karlsson, B. Lee, T. Åkermark, T. E. V. Johnston, M. D. Kärkäs, J. Sun, Ö. Hansson, J. Bäckvall and B. Åkermark, *Angew. Chem. Int. Ed.* 2011, **123**, 11919

6 R. K. Hocking, R. Brimblecombe, L. -Y. Chang, A. Singh, M. H. Cheah, C. Glover, W. H. Casey and L. Spiccia, *Nat. Chem.*, 2011, **3**, 461; M. M. Najafpour and A. Nemati Moghaddam, *Dalton Trans.,* 2012, **41**, 10292; M. M. Najafpour and V. McKee, *Catal. Commun.*, 2010, **11**, 1032; M. M. Najafpour, B. Kozlevcar, V. McKee, Z. Jaglicic and M. Jagodic, *Inorg. Chem. Commun.*, 2011, **14**, 125; M. M. Najafpour, W. Hillier, A. N. Shamkhali, M. Amini, K. Beckmann, Z. Jagličić, M. Jagodic, P. Strauch, A. Nemati Moghaddam, G. Berettai and M. Bagherzadeh, *Dalton Trans.,* 2012, **41**, 12282.

7 T. S. Glikman and I. S. Shcheglova, Kinetika i Kataliz. 1968, **9**, 461.

8 M. Morita, C. Iwakura and H. Tamura, *Electrochim. Acta*, 1977, **22**, 325.

9 V. Shaflrovich, V. Ya. and A. E. Shilov, *Kinet Katal.,* 1978, **19**, 877.

10 A. Harriman, I. J. Pickering, J. M. Thomas and P. A. Christensen, *J. Chem. Soc., Faraday Trans*. 1, 1988, **84**, 2795.

11 M. M. Najafpour, *Origins Life Evol. Biosph*., 2011, **41**, 237; M. M. Najafpour, *Geomicrobiol. J*., 2011, **28**, 714; M. M. Najafpour, M. Amouzadeh Tabrizi, B. Haghighi and Govindjee, *Dalton Trans.,* 2012, **41**, 3906; M. M. Najafpour, M. Amouzadeh Tabrizi, B. Haghighi and Govindjee, *Dalton Trans.,* 2013, **42**, 879; M. M. Najafpour, *Chem. Commun*., 2011, **47**, 11724; M. M. Najafpour, *J. Photochem. Photobiol. B*, 2011, **104**, 111; M. M. Najafpour, D. Jafarian Sedigh, C. K. King'ondu and S. L. Suib, *RSC Adv*., 2012, **2**, 11253; A. Singh, R. K. Hocking, S. L. Y. Chang, B. M. George, M. Fehr, L. Klaus, A. Schnegg and L. Spiccia, *Chem. Mater.*, 2013, **25**, 1098; F. Zhou, A. Izgorodin, R. K. Hocking, V. Armel, L. Spiccia and D. R. MacFarlane, *ChemSusChem*, 2013, **6**, 643; A. Schöler, I. Zaharieva, S. Zimmermann, M. Wiechen, A. Manke, P. Kurz, C. Plieth and H. Dau, *Eur. J. Inorg. Chem*., 2014, **4**, 680; I. Zaharieva, P. Chernev, M. Risch, K. Klingan, M. Kohlhoff, A. Fischer and H. Dau, *Energ. Environ. Sci*., 2012, **5**, 7081; A. Indra, P. W. Menezes, I. Zaharieva, E. Baktash, J. Pfrommer, M. Schwarze, H. Dau, M. Driess, *Angew. Chem. Int. Ed*., 2013, **52**, 13206; D. M. Robinson, Y. B. Go, M. Mui, G. Gardner, Z. Zhang, D. Mastrogiovanni, E. Garfunkel, J. Li, M. Greenblatt and G. C. Dismukes, *J. Am. Chem. Soc.*, 2013, **135**, 3494.

12 M. M. Najafpour, F. Rahimi, D. J. Sedigh, R. Carpentier, J. J. Eaton-Rye, J. -R. Shen and S. I. Allakhverdiev, *Photosyn. Res.*, 2013, **117**, 423; Y. Gorlin, C. -J. Chung, J. D. Benck, D. Nordlund, L. Seitz, T.-C. Weng, D. Sokaras, B. M. Clemens and T. F. Jaramillo, *J. Am. Chem. Soc*., 2014, **136**, 4920

13 F. Jiao and H. Frei, *Chem. Commun*., 2010, **46**, 2920.

14 D. M. Robinson, Y. B. Go, M. Mui, G. Gardner, Z. Zhang, D. Mastrogiovanni, E. Garfunkel, J. Li, M. Greenblatt and G. C. Dismukes, *J. Am. Chem. Soc*., 2013, **135**, 3494.

15 M. M. Najafpour and D. Jafarian Sedigh, *Dalton Trans*., 2013, **42**, 12173; M. M. Najafpour, B. Haghighi, D. Jafarian Sedigh and M. Zarei Ghobadi, *Dalton Trans*., 2013, **42**, 16683.

16 M. M. Najafpour, M. Kompany-Zareh, A. Zahraei, D. J. Sedigh, H. Jaccard, M. Khoshkam, R. D. Britt and W. H. Casey, *Dalton Trans.*, 2013, **42**, 14603; R. K. Hocking, R. Brimblecombe, L.-Y. Chang, A. Singh, M. H. Cheah, C. Glover, W. H. Casey and L. Spiccia, *Nat. Chem.*, 2011, **3**, 461; M. M. Najafpour, A. N. Moghaddam, H. Dau and I. Zaharieva, *J. Am. Chem. Soc*., 2014, **136**, 7245. R. K. Hocking, R. Malaeb, W. P. Gates, A. F. Patti, S. L. Y. Chang, G. Devlin, D. R. MacFarlane and L. Spiccia, *ChemCatChem*., 2014, **6**, 2028; M. M. Najafpour, M. Holynska, A. N. Shamkhali, S. H. Kazemi, W. Hillier, E. Amini, M. Gaemmaghami, D. J. Sedigh, A. N. Moghaddam, R. Mohamadi, S. Zaynalpoor and K. Beckmann, *Dalton Trans*., 2014, **43**, 13122.

17 M. M. Najafpour, F. Rahimi, M. Fathollahzadeh, B. Haghighi, M. Holynska, T. Tomo and S. I. Allakhverdiev, *Dalton Trans*., 2014, **43**, 10866; M. M. Najafpour, M. Abasi, T. Tomo and S. I. Allakhverdiev, *Dalton Trans*., 2014, **43**, 12058; M. M. Najafpour, M. Abasi, T. Tomo and S. I. Allakhverdiev, *RSC Adv*., 2014, 2014,**4**, 37613.

18 T. Takashima, K. Hashimoto and R. Nakamura, *J. Am. Chem. Soc.,* 2012, **134**, 18153.

19 A. Yamaguchi, R. Inuzuka,T. Takashima,T. Hayashi, K. Hashimoto an R. Nakamura, *Nat. Commun*., 2014, **5**, 4256.

20 M. Huynh, D. K. Bediako and D. G. Nocera, *J. Am. Chem. Soc.*, 2014, **136**, 6002.

21 J. R. Kona, C. K. King'ondu, A. R. Howell and S. L. Suib, *ChemCatChem*, 2014, **6**, 749.

22 D. Rawtani and Y. K. Agrawal, *Rev. Adv. Mater. Sci*., 2012, **30**, 282; M. Du, B. Guob and D. Jia, *Polym. Int*., 2010, **59**, 574; S. Chen1, J. Li, Y. Zhang, D. Zhang and J. Zhu, J. Natur. Gas Chem., 2012, **21**, 426; D. Rawtani, R. Deepak and Y. K. Agrawal, *Emerging Mat. Res.*, 2012, **1**, 212; D. G. Shchukin, G. B. Sukhorukov, R. R. Price and Y. M. Lvov, *Small*, 2005, **1**, 510.

23 a) S. Bordeepong, D. Bhongsuwan, T. Pungrassami and T. Bhongsuwan, *J. Sci. Technol*., 2011, **33** (5), 599; b) H. W. Nesbitt and D. Banerjee, *Amer. Miner.,* 1998, **83**, 305.

24 C. E. Frey, M. Wiechen and P. Kurz, *Dalton Trans*., 2014, **43**, 4370.

25 M. M. Najafpour, B. Pashaei, *Dalton Trans*., **41**, 2012, 10156.

26 M. M. Najafpour, S. Nayeri and B. Pashaei, *Dalton Trans.*, 2011, **40**, 9374.

27 M. M. Najafpour, D. J. Sedigh, B. Pashaei and S. Nayeri, *New J. Chem.*, 2013, **37**, 2448.

28 M. M. Najafpour, B. Pashaei and S. Nayeri, *Dalton Trans*., 2012, **41**, 7134.

29 M. M. Najafpour, M. Abasi and M. Hołyńska, *RSC Adv*., 2014, **4**, 36017.

30 M. M. Najafpour, T. Ehrenberg, M. Wiechen and P. Kurz, *Angew. Chem. Int. Ed.*, 2010, **49**, 2233.

31 A. Iyer, J. Del-Pilar, C. Kithongo King'ondu, E. Kissel, H. Fabian Garces, H. Huang, A. M. El-Sawy, P. K. Dutta and S. L. Suib, *J. Phys. Chem.* C, 2012, **116**, 6474.

32 M. M. Najafpour and E. Amini, *Dalton Trans.*, 2015, **44**, 1039.

33 Y. Okuno, O. Yonemitsu and Y. Chiba, *Chem. Lett*., 1983, 815.

34 M. M. Najafpur, R. Mostafalu and B. Kaboudin, *J. Photochem. Photobiol. B*, Submitted Manuscript,

35 M. M. Najafpour and A. N. Moghaddam, *New J. Chem.*, 2012, **36**, 2514.

36 M. M. Najafpour, *Dalton Trans*., 2011, **40**, 3805.

37 V. B. R. Boppana and F. Jiao, *Chem. Commun*., 2011, **47**, 8973.

38 M. M. Najafpour, *Dalton Trans*., 2011, **40**, 3793.

39 M. M. Najafpour, S. Nayeri and B. Pashaei, *Dalton Trans*., 2012, **41**, 4799.

40 D. M. Robinson, Y. B. Go, M. Greenblatt and G. C. Dismukes, *J. Am. Chem. Soc.,* 2010, **132**, 11467.

41 C. W. Cady, R. H. Crabtree and G. W. Brudvig, *Coord. Chem. Rev*., 2008, **252**, 444.

42 R. Ramaraj, A. Kira and M. Kaneko, *Angew. Chem.,* 1986, **98**, 824.

43 G. C. Dismukes, R. Brimblecombe, G. A. N. Felton, R. S. Pryadun, J. E. Sheats and L. Spiccia, G. F. Swiegers, *Acc. Chem. Res.*, 2009, **42**, 1935.

44 G. Ananyev and G. C. Dismukes, *Photosynth. Res.*, 2005, **84**, 355.

45 P. Liu and M. Zhao, *Appl. Surf. Sci.*, 2009, **255**, 3989; L. Wang, J. Chen, L. Ge, Z. Zhu and V. Rudolph, *Energy Fuels*, **25**, 3408; R. Zhai, B. Zhang, L. Liu, Y. Xie, H. Zhang and J. Liu, *Cat. Commun.*, **12**, 259; Y. Zhang and H. Yang, *Phys. Chem. Miner.*, **39**, 789; R. Wang, G. Jiang, Y. Ding, Y. Wang, X. Sun, X. Wang and W. Chen, *ACS Appl. Mater. Interfaces*, **3**, 4154; Z.-Y. Cai, M.-Q. Zhu, H. Dai, Y. Liu, J.-X. Mao, X.-Z. Chen and C.-H. He, *Adv. Chem. Eng. Sci.*, 2011, **1**, 15; D. Zhang, W. Huo, J. Wang, T. Li, X. Cheng, J. Li and A. Zhang, *J. Appl. Poly. Sci.*, 2012, **126**, 1580.

46 Critical raw materials for the E, Report of the Ad-hoc Working Group on defining critical raw materials, European Commission 2010.

47 Studie des IZT und ISI im Auftrag des BMWi, Schlussbericht: Rohstoffe für Zukunftstechnologien 2009.

| Compound | Oxidant | TOF mmol $O_2$/mol Mn.s | References |
|---|---|---|---|
| Nano-sized Mn oxide on halloysite | Ce(IV) | 1.5-2.8 | This work |
| Nano scale Mn oxide within NaY zeolite | Ce(IV) | 2.62 | 25 |
| Layered Mn-Ca oxide | Ce(IV) | 2.2 | 24,26 |
| Layered Mn-Al, Zn, K, Cd and Mg oxide | Ce(IV) | 0.8-2.2 | 27, 28 |
| Layered Ni(II) oxide | Ce(IV) | 0.4-0.6 | 29 |
| $CaMn_2O_4.H_2O$ | Ce(IV) | 0.54 | 30 |
| Amorphous Mn Oxides | $Ru(bpy)_3^{3+}$ | 0.06 | 31 |
|  | Ce(IV) | 0.52 |  |
| Nano-sized Mn oxide on high surface (high surface) montmorillonite | Ce(IV) | 0.5 | This work |
| Nanolayered Mn oxide | Ce(IV) | 0.45 | 32 |
| $CaMn_2O_4.4H_2O$ | Ce(IV) | 0.32 | 30 |
| Mn oxide nanoclusters | $Ru(bpy)_3^{3+}$ | 0.28 | 33 |
| β-MnO(OH) | CAN | 0.24 | 34 |
| Mn oxide-coated montmorillonite (low surface) | Ce(IV) | 0.22 | 35 |
| Layered Mn-Cu(II) | Ce(IV) | 0.2-0.35 | 29 |
| $Mn_3O_4$ | CAN | 0.01-0.17 | 34 |
| Octahedral Molecular Sieves | $Ru(bpy)_3^{3+}$ | 0.11 | 31 |
|  | Ce(IV) | 0.05 |  |
| $MnO_2$ (colloid) | Ce(IV) | 0.09 | 36 |
| $\alpha$-$MnO_2$ nanowires | $Ru(bpy)_3^{3+}$ | 0.059 | 37 |
| $CaMn_3O_6$ | Ce(IV) | 0.046 | 38 |
| $CaMn_4O_8$ | Ce(IV) | 0.035 | 39 |
| $\alpha$-$MnO_2$ nanotubes | $Ru(bpy)_3^{3+}$ | 0.035 | 37 |
| $Mn_2O_3$ | Ce(IV) | 0.027 | 30 |
| $\beta$-$MnO_2$ nanowires | $Ru(bpy)_3^{3+}$ | 0.02 | 37 |
| $Ca_2Mn_3O_8$ | Ce(IV) | 0.016 | 39 |
| $CaMnO_3$ | Ce(IV) | 0.012 | 39 |
| Nano-sized $\lambda$-$MnO_2$ | $Ru(bpy)_3^{3+}$ | 0.03 | 40 |
| Bulk $\alpha$-$MnO_2$ | $Ru(bpy)_3^{3+}$ | 0.01 | 37 |
| Mn Complexes | Ce(IV) | 0.01-0.6 | 41,42 |
| PSII | Sunlight | 100-400 × $10^3$ | 43,44 |